On the Ultra-Reliable and Low-Latency Communications in Flexible TDD/FDD 5G Networks

Esswie, Ali Abdelmawgood Ali Ali; Pedersen, Klaus Ingemann

Published in:
2020 IEEE 17th Annual Consumer Communications & Networking Conference (CCNC)

DOI (link to publication from Publisher):
10.1109/CCNC46108.2020.9045657

Publication date:
2020

Document Version
Accepted author manuscript, peer reviewed version

On the Ultra-Reliable and Low-Latency Communications in Flexible TDD/FDD 5G Networks

Ali A. Esswie[1,2], *Member, IEEE*, and Klaus I. Pedersen[1,2], *Senior Member, IEEE*
[1]Nokia Bell-Labs, Aalborg, Denmark
[2]Department of Electronic Systems, Aalborg University, Denmark

***Abstract*—The ultra-reliable and low-latency communication (URLLC) is the key driver of the current 5G new radio standardization. URLLC encompasses sporadic and small-payload transmissions that should be delivered within extremely tight radio latency and reliability bounds, i.e., a radio latency of 1 ms with 99.999% success probability. However, such URLLC targets are further challenging in the 5G dynamic time division duplexing (TDD) systems, due to the switching between the uplink and downlink transmission opportunities and the additional inter-cell cross-link interference (CLI). This paper presents a system level analysis of the URLLC outage performance within the 5G new radio flexible TDD systems. Specifically, we study the feasibility of the URLLC outage targets compared to the case with the 5G frequency division duplexing (FDD), and with numerous 5G design variants. The presented results therefore offer valuable observations on the URLLC outage performance in such deployments, and hence, introducing the state-of-the-art flexible-FDD technology.**

***Index Terms*— Dynamic-TDD; Flexible-FDD; 5G new radio; URLLC; Cross link interference (CLI).**

I. Introduction

The fifth generation (5G) new radio (NR) is designed to support a variety of services such as ultra-reliable and low-latency communications (URLLC) [1], industrial time sensitive communications (TSC) [2], and enhanced mobile broadband (eMBB) communications [3]. Those come with challenging requirements for the packet latency, jitter, and aggregated capacity, respectively. On another side, dynamic time division duplexing (TDD) is the major duplexing technology for 5G NR due to the wide spectrum availability of unpaired bands, i.e., the 3.5 GHz band, and spectrum above 6 GHz [4]. Additionally, the frequency division duplexing (FDD) is also supported for 5G NR, and considered especially relevant for deployments at bands below 6 GHz [5]. In this regard, fulfilling the URLLC requirements for FDD systems is obviously more manageable since both base-stations (BSs) and user-equipments (UEs) always have simultaneous uplink (UL) and downlink (DL) transmission opportunities.

Although, for TDD deployments, it is further challenging to fulfill such targets due to the restriction of either having exclusively UL or DL transmissions. Hence, in a multi-cell multi-user scenario, it becomes a hard problem to ensure that the URLLC latency and reliability requirements are met for all active UEs, as the inter-UE timing relations may likely be different. It is therefore a non-trivial problem how to dynamically adjust the UL-DL switching for 5G NR TDD.

The standardization body has accordingly defined a flexible slot format design [6], where the traffic adaptation could occur per 14-OFDM symbol slots. In principle, such a design allows BSs to dynamically adapt their link directions, i.e., UL or DL symbols, according to a local selection criterion such as the buffered traffic statistics (incl. e.g., the related head of line delay). Although, when different neighboring BSs concurrently adopt opposite transmission link directions, it comes with the cost of potentially severe cross-link interference (CLI) [7]. CLI is highly critical for achieving the URLLC outage requirements, where especially the BS-BS CLI is problematic due to the higher BS transmit power as compared to the UE transmit powers. Accordingly, the majority of the recent TDD studies tackled the CLI issue either by pre-avoidance or post-cancellation techniques. In [8], coordinated inter-cell user scheduling, and advanced UL power control are introduced to minimize the average network CLI. Furthermore, opportunistic frame coordination schemes [7, 9] are proposed to pre-avoid the occurrence of the BS-BS and UE-UE CLI on a best-effort basis. Moreover, perfect BS-BS CLI cancellation using full packet exchange and orthogonal projector estimation are discussed in [10, 11].

In this paper, we study the URLLC outage performance in an advanced system-level setting with high degree of realism. Particularly, how to most efficiently manage the switching between the UL and DL transmission opportunities to best meet the URLLC traffic conditions is investigated, assuming bi-directional random time-variant traffic. The impact of adjusting the TDD switching pattern at different time-resolutions is analyzed, including a sensitivity analysis for other system-level parameter settings and algorithm variants. For dynamic TDD, we isolate the effect of the CLI by presenting both cases where the CLI is realistically modeled, in addition to the case where an optimal CLI cancellation is assumed. To the best of our knowledge, no prior studies have presented such system-level URLLC outage results and related recommendations for 5G NR TDD deployments.

This paper is organized as follows. Section II discusses the system modeling. Section III introduces the URLLC radio latency analysis in dynamic-TDD systems, while Section IV presents our adaptation criterion of the dynamic link selection. The URLLC outage latency assessment is introduced in Section V. Finally, the flexible-FDD duplexing mode is discussed in Section VI, while conclusions appear in Section VII.

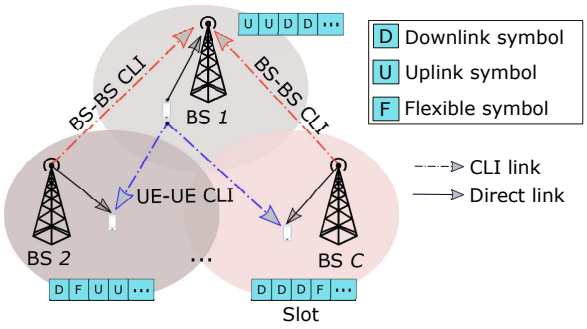

Fig. 1. Dynamic-TDD deployment per slot periodicity.

II. System Modeling

We consider a 5G-NR dynamic TDD macro network with C BSs, each with N_t antennas, where there are K^{dl} and K^{ul} uniformly-distributed DL and UL active UEs per BS, each with M_r antennas. We assume inter-BS synchronized TDD transmissions, as depicted in Fig. 1. Additionally, the URLLC-alike sporadic FTP3 traffic model is adopted with the packet sizes of f^{dl} and f^{ul} bits, and Poisson Point Processes, with mean packet arrivals λ^{dl} and λ^{ul}, in the DL and UL directions, respectively. Thus, the average offered traffic load per BS in the DL direction is expressed as: $\Omega^{\text{dl}} = K^{\text{dl}} \times f^{dl} \times \lambda^{\text{dl}}$, and in the UL direction as: $\Omega^{\text{ul}} = K^{\text{ul}} \times f^{ul} \times \lambda^{\text{ul}}$. The total offered load per BS is: $\Omega = \Omega^{\text{dl}} + \Omega^{\text{ul}}$.

We adopt the state-of-the-art 3GPP 5G-NR configurations. UEs are multiplexed using the orthogonal frequency division multiple access (OFDMA), and with 30 kHz sub-carrier spacing (SCS). The smallest resource unit, granted to an active UE, is the physical resource block (PRB) of 12 consecutive SCs. The dynamic user scheduling is applied per a TTI duration of 4-OFDM symbols, for faster URLLC transmissions.

III. URLLC Radio Latency Analysis

The 3GPP 5G-NR release-15 standard has defined several slot format designs [6]. A slot format denotes a certain placement of the DL [D], UL [U], and flexible [F], OFDM symbols within a slot duration of 14 OFDM symbols. The flexible symbols imply that these could be used either for UL/DL transmissions or as guard intervals between consecutive DL and UL symbols. The average one-way URLLC latency in the DL direction Ψ_{dl} is given by

$$\Psi_{\text{dl}} = \Lambda_{\text{bsp}} + \psi_{\text{tq}} + \psi_{\text{fa}} + \psi_{\text{tti}} + \alpha\psi_{\text{harq}} + \Lambda_{\text{uep}}, \quad (1)$$

where Λ_{bsp}, ψ_{tq}, ψ_{fa}, ψ_{tti}, ψ_{harq} and Λ_{uep} denote the BS processing, DL total queuing, DL frame alignment, DL packet transmission, DL hybrid automatic repeat request (HARQ) re-transmission, and UE processing delays, respectively. α implies the target block error rate (BLER), e.g., for a URLLC-alike BLER = 1%, $\alpha = 0.01$, and $\alpha = 0$ if the packet has been successfully decoded from the first transmission. As can be observed, Λ_{bsp}, ψ_{tti} and Λ_{uep} impose a constant delay offset, and are only dependent on the UE/BS processing capabilities, and TTI size, respectively; however, ψ_{tq} and ψ_{harq} are time-varying DL delay components, depending on the DL offered load level, DL and UL link switching delay, and the inflicted DL interference, respectively.

Accordingly, the DL HARQ delay ψ_{harq} is expressed as

$$\psi_{\text{harq}} = \Lambda_{\text{uep}} + \varphi_{\text{fa}} + \varphi_{\text{nack}} + \Lambda_{\text{bsp}} + \psi_{\text{tq}} + \psi_{\text{fa}} + \psi_{\text{tti}}, \quad (2)$$

where φ_{fa} implies the alignment delay towards the first UL control channel opportunity for the UE to transmit the HARQ negative acknowledgment (NACK), with φ_{nack} as the NACK transmission time. The summation $\varphi_{\text{fa}}+\varphi_{\text{nack}}+\Lambda_{\text{bsp}}$ represents the total delay from the time a UE has identified a corrupted DL packet until the BS becomes aware of it. Subsequently, the total DL queuing delay ψ_{tq} is calculated by

$$\psi_{\text{tq}} = \psi_{\text{q}} + \psi_{\text{tdd}}, \quad (3)$$

where ψ_{q} implies the packet queuing delay due to the dynamic multi-user scheduling, and ψ_{tdd} is TDD UL-DL link-switching delay, i.e., the additional DL buffering delay towards the first available DL transmission symbol(s) due to the non-concurrent DL and UL transmission availability. For instance, with FDD, $\psi_{\text{tdd}} = 0$ ms. Fig. 2a shows an example of the factors which contribute to the average one-way DL latency Ψ_{dl}, where a single DL packet associated with one HARQ re-transmission is assumed. As can be observed, the DL packet is decoded at its intended UE after 22 OFDM-symbol duration, i.e., 0.7 ms, from its arrival time at the BS, satisfying the URLLC 1-ms radio latency target; however, with the assumption of immediate DL scheduling and transmission once the packet arrives the BS DL buffer, i.e., $\psi_{\text{td}} = 0$.

Similarly, the one-way URLLC UL latency Ψ_{ul} follows a similar behavior as Ψ_{dl}; however, with a linear delay offset due to the UL scheduling. Specifically, with dynamic-grant (DG) UL scheduling, UEs first align to the first available transmission opportunity of the UL control channel, i.e., φ_{fa}, in order to send the scheduling request (SR), and accordingly wait for the scheduling grant (SG) from the serving BS over the DL control channel. Thus, Ψ_{ul} is given by

$$\Psi_{\text{ul}} = \varphi_{\text{dg}} + \varphi_{\text{td}} + \varphi_{\text{fa}} + \varphi_{\text{tti}} + \alpha\varphi_{\text{harq}} + \Lambda_{\text{bsp}}, \quad (4)$$

where φ_{dg}, φ_{td}, φ_{fa}, φ_{tti} and φ_{harq} are the UL DG delay, UL total buffering delay, UL frame alignment delay, UL payload transmission delay, and UL HARQ delay, respectively.

On another side, the grant-free (GF) UL scheduling [12] is considered as vital for URLLC UL transmissions. With UL grant-free, sporadic UL packets become immediately eligible for scheduling and transmission, i.e., no SR and SG delays, $\varphi_{\text{dg}} = \varphi_{\text{sr}} = \psi_{\text{sg}} = 0$ ms, with φ_{sr} and ψ_{sg} as the transmission delays of the SR and SG, respectively; although, with the DG, φ_{dg} is then calculated as

$$\varphi_{\text{dg}} = \Lambda_{\text{uep}} + \varphi_{\text{fa}} + \varphi_{\text{sr}} + \Lambda_{\text{bsp}} + \psi_{\text{fa}} + \psi_{\text{sg}} + \Lambda^{'}_{\text{uep}}, \quad (5)$$

with $\Lambda^{'}_{\text{uep}}$ as the UE processing delay to decode the SG, i.e., Λ_{uep}, as well as preparing the UL transport block, where $\Lambda^{'}_{\text{uep}} > \Lambda_{\text{uep}}$.

Equivalently to (2) and (3), the UL HARQ φ_{harq} and total queuing φ_{td} delays are given by

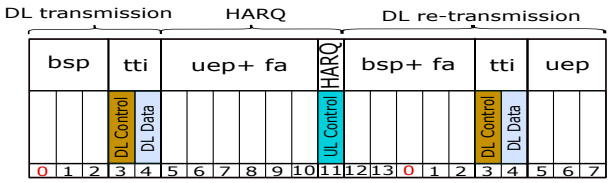

(a) Latency of a single DL packet arrival.

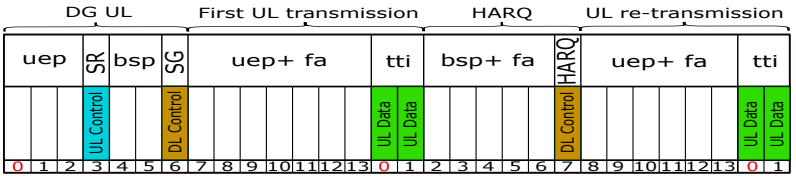

(b) Latency of a single UL packet arrival, with DG UL scheduling.

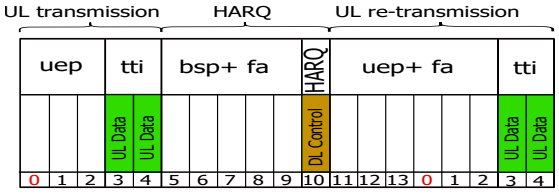

(c) Latency of a single UL packet arrival, with GF UL scheduling.

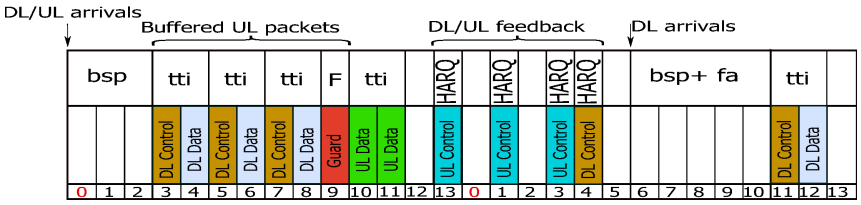

(d) Latency of multiple UL and DL packet arrivals.

Fig. 2. URLLC one-way latency components with DG, and GF UL, for a TTI size = 2-OFDM symbols, and SCS = 30 kHz.

$$\varphi_{\text{harq}} = \Lambda_{\text{bsp}} + \psi_{\text{fa}} + \psi_{\text{nack}} + \Lambda_{\text{uep}} + \varphi_{\text{td}} + \varphi_{\text{fa}} + \varphi_{\text{tti}}. \quad (6)$$

$$\varphi_{\text{td}} = \varphi_{\text{q}} + \varphi_{\text{tdd}}, \quad (7)$$

where φ_{q} and φ_{tdd} denote the UL packet queuing delay and the delay towards the first available UL transmission opportunity, where $\varphi_{\text{td}} \neq \psi_{\text{td}}$ due to the different UL and DL offered load, leading to varying UL and DL buffering performance, respectively. Fig. 2b and 2c depict the radio latency components which affect the average one-way URLLC UL latency Ψ_{ul}, for the DG and GF UL scheduling cases, respectively, and under the assumption of a single UL packet arrival without further multi-UE queuing delays. With the UL DG and one UL HARQ re-transmission, the URLLC UL packet gets delivered after 30-OFDM symbol duration, i.e., 1 ms, which does not allow for any further packet buffering due to the dynamic user scheduling; otherwise, the URLLC UL 1-ms latency target shall be violated.

Finally, Fig. 2d presents an example of multiple concurrent DL and UL packet arrivals, unlike Fig. 2a, 2b, and 2c, respectively. Herein, the BS decides multiple DL TTIs first to transmit the early-arriving DL packets. Accordingly, the UL packets are buffered over those DL TTIs as well as several guard symbols towards the first available UL TTI opportunity, i.e., $\varphi_{\text{tdd}} \ggg 0$ ms, exceeding the UL latency budget. Next, the BS adopts alternating DL and UL TTI instances for the subsequent DL/UL HARQ feedback.

IV. Traffic Adaptation in Dynamic-TDD Systems

For a dynamic TDD deployment, BSs dynamically match their transmission link directions to the sporadic traffic arrivals. Hence, at each pattern update periodicity, which could be either per a slot or aggregated several slots, BSs select the slot formats, i.e., number of DL and UL symbols during the next slot(s), which best satisfy their individual link direction selection criteria. We consider the amount of buffered DL and UL traffic to select the link directions. Thus, we define the buffered traffic ratio ϖ_c as

$$\varpi_c = \frac{Z_c^{\text{dl}}}{Z_c^{\text{dl}} + Z_c^{\text{ul}}}, \quad (8)$$

where Z_c^{dl} and Z_c^{ul} are the aggregated buffered traffic size in the DL and UL directions, respectively. Herein, we assume perfect knowledge of Z_c^{ul} at the BSs from the UEs buffer status reports and pending SRs, respectively. The lower ϖ_c ratio, the larger the buffered UL traffic volume, and thus, BSs select slot formats with a majority of UL symbols. For instance, at an

Table I
DEFAULT SIMULATION PARAMETERS.

Parameter	Value
Environment	3GPP-UMA, one cluster, 21 cells
UL/DL channel bandwidth	20 MHz, SCS = 30 KHz, TDD
Antenna setup	$N_t = 4$, $M_r = 4$
UL power control	$\alpha = 1$, $P0 = -103$ dBm
Link adaptation	Adaptive modulation and coding
UE processing time	DL : 4.5/9-OFDM symbols UL : 5.5/11-OFDM symbols
Average user load per cell	$K^{\text{dl}} = K^{\text{ul}} = 1$, 10, 50, 100 and 200
TTI configuration	4-OFDM symbols
Traffic model	FTP3 $f^{dl} = f^{ul}$ = 400 bits $\lambda^{\text{ul}} = \lambda^{\text{dl}}$ = 100 pkts/sec
Interference conditions	Interference-free
DL/UL scheduling	Proportional fair; UL GF [12]
DL/UL receiver	LMMSE-IRC
Pattern update periodicity	1 radio frame (10 ms)

arbitrary BS with $\varpi_c = 0.2$, the buffered UL traffic volume is 4x the buffered DL traffic, thus, BS consequently selects a slot format of DL:UL symbol ratio as $\sim 1:4$. In case there are neither new packet arrivals nor buffered traffic at an arbitrary time instant, BSs fall back to a default slot format with equal DL and UL symbol share; however, BSs do not schedule any UEs though. This way, BSs tend to rapidly adapt to the accumulating buffered traffic, equalizing both the DL and UL TDD queuing performance, i.e., ψ_{tdd} and φ_{tdd}.

In this work, the order of the DL and UL OFDM symbols during the adopted slot format(s) is evenly distributed with a block size of 4 symbols, e.g., a selected slot pattern of $\sim 2:1$ DL:UL symbol ratio is configured as: [DDDDFU-UUUDDDDF]. Such configuration allows for alternating DL and UL transmission opportunities during each slot duration for urgent packet arrivals; however, it comes at the expense of inflicting more guard symbols, i.e., [F] symbols, among each DL and UL symbol pair.

V. URLLC OUTAGE LATENCY ASSESSMENT

We evaluate the URLLC radio performance using inclusive system level simulations [7], where the major functionalities of the physical and media access control layers, respectively, are implemented according to the latest 5G-NR specifications. The default simulation assumptions are listed in Table I, unless otherwise mentioned. We consider asynchronous Chase-combining HARQ, where the HARQ re-transmissions are dynamically scheduled and always prioritized over new transmissions. Finally, the URLLC outage latency, i.e., radio latency at the 10^{-5} outage probability, is assessed under various 5G system configurations.

URLLC outage latency with pattern update periodicity γ:

The pattern update periodicity implies how frequent the BSs update their corresponding slot formats, hence, how fast they adapt the network capacity towards the sporadic DL/UL packet arrivals. For instance, $\gamma = 1$ slot denotes that BSs update their adopted DL and UL symbol patterns per every slot duration, i.e., 14 OFDM symbols. Fig. 3 holds a comparison of the DL/UL combined URLLC outage latency under FDD, TDD with $\gamma = 1$ slot and a single frame duration, respectively, and

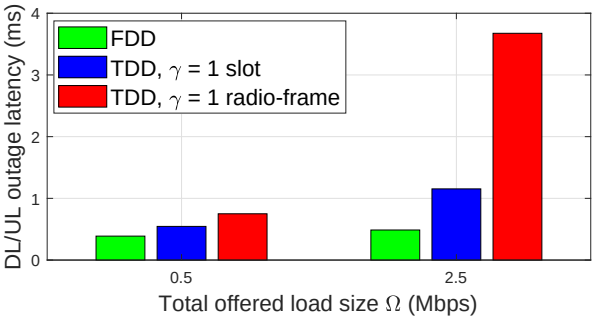

Fig. 3. URLLC outage latency: with γ.

for 20 MHz bandwidth. An equivalent FDD bandwidth allocation is also adopted, i.e., 10 MHz for UL transmissions and 10 MHz for DL transmissions. As can be clearly seen, at the lower load, i.e., $\Omega = 0.5$ Mbps, both duplexing schemes under evaluation achieve the 1-ms URLLC latency target. Although, by increasing the offered load up to $\Omega = 2.5$ Mbps, the FDD significantly outperforms the respective TDD, in terms of the URLLC outage latency due to the immediate availability of the DL and UL capacity, i.e., no TDD delays inflicted, and hence, $\psi_{\text{tdd}} = \varphi_{\text{tdd}} = 0$ ms. Accordingly, the TDD with a $\gamma = 1$ slot achieves a greatly improved URLLC outage latency, i.e., -218.7% outage latency reduction compared to the case of $\gamma = 1$ radio-frame, because of the faster link adaptation to the random DL/UL packet arrivals, leading to less traffic buffering delays. However, this comes with a significantly increased control overhead size, due to the guard time duration between each consecutive DL and UL symbol pair.

URLLC outage latency with dynamic and grant-free UL:

Based on the latency analysis in Section III, grant-free UL has been demonstrated to significantly reduce the URLLC UL outage latency, compared to DG. Accordingly, Fig. 4 depicts the complementary cumulative distribution function (CCDF) of the URLLC DL/UL combined latency when UL grant-free and DG are adopted. Herein, with DG UL, UEs transmit the scheduling request on a periodicity of 16 TTIs, and hence, receive the corresponding scheduling grant 4 TTIs later. As noticed, the DG UL exhibits a linear offset in the UL outage latency by the additional latency component φ_{dg}, leading to $\sim +400\%$ increase in the URLLC outage latency, compared to the GF UL case, with $\varphi_{\text{dg}} = 0$ ms.

URLLC outage latency with the SCS size ρ:

The size of the channel SCS has a critical impact on the URLLC outage latency. Unlike the 4G standards, the 5G-NR specs adopt different SCSs for its diverse service classes, i.e., $\rho = 15$, 30, and 60 kHz, respectively, for the carrier frequencies below 6 GHz. However, it was recently agreed within the 3GPP community that $\rho = 15$ kHz is no longer appropriate for URLLC transmissions. Accordingly, the achievable URLLC UL outage latency with the SCS size is presented in Fig. 5, for different offered loads Ω. The larger SCS size, i.e., $\rho = 60$ kHz, offers: (a) reduced BS and UE processing delays, i.e., Λ_{bsp} and Λ_{uep}, due to the shorter OFDM symbols in time, and (2) a higher probability of non-segmented URLLC transmissions, i.e., URLLC payload is transmitted in a single-shot without segmentation, reducing the DL ψ_{q} and

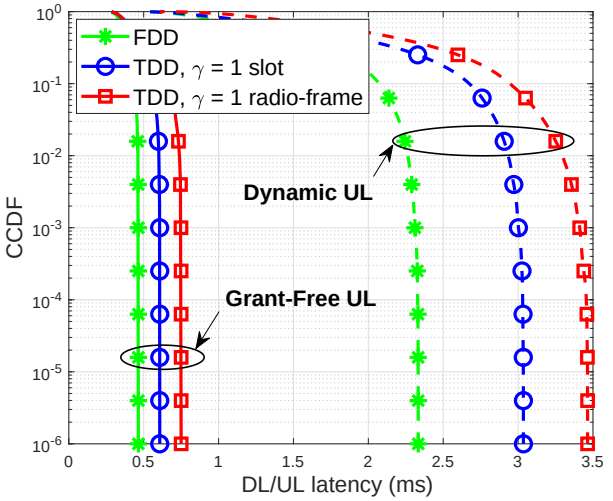

Fig. 4. URLLC outage latency: with DG, GF, $\Omega = 0.5$ Mbps.

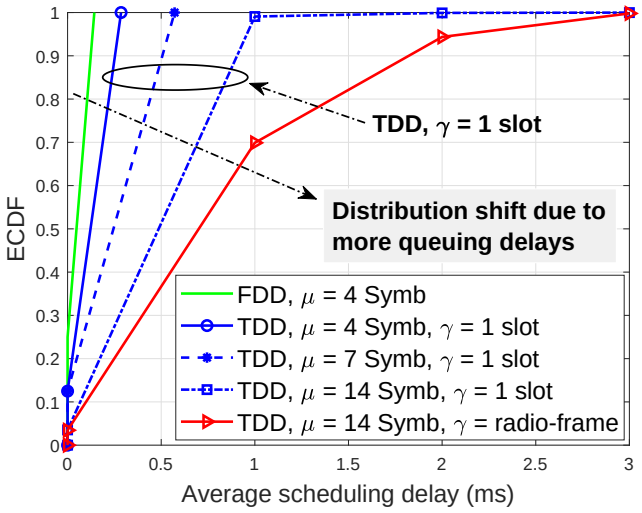

Fig. 6. URLLC outage latency: with μ, $\Omega = 1$ Mbps.

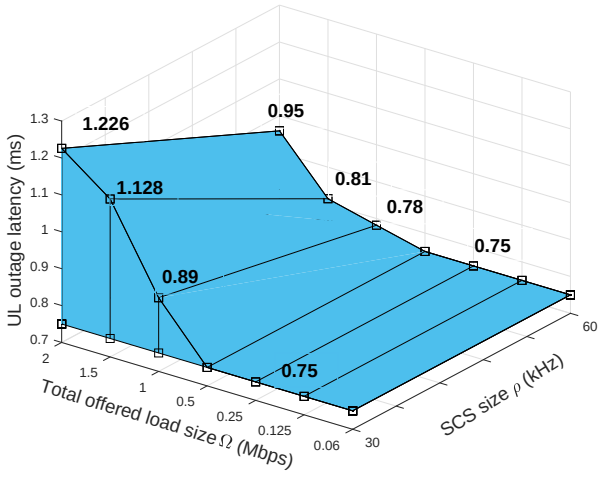

Fig. 5. URLLC UL outage latency: with ρ.

UL φ_{q} buffering delays, respectively. Accordingly, a larger ρ allows for faster URLLC transmissions to compensate for the additional DL and UL switching delay of the dynamic-TDD systems, satisfying the stringent URLLC 1-ms outage latency.

URLLC outage latency with the TTI size μ:

The TTI length determines the packet transmission periodicity. Hence, it has a key impact on the maximum alignment delay that an arbitrary packet may inflict until the first available DL/UL TTI instance. As shown in Fig. 6, the empirical CDF (ECDF) of the average scheduling delay of the combined DL ψ_{td} and UL φ_{td} transmissions, is introduced for $\mu = 4, 7,$ and 14 OFDM symbols, respectively. Hence, the scheduling delay defines the delay between the time instant a packet arrives at the scheduling buffers until it is being transmitted, excluding the processing times. Obviously, the larger μ, the larger the time delay of which the incoming packets shall exhibit in the scheduling buffers. The TDD case with $\gamma = 1$ radio-frame and $\mu = 14$ OFDM symbols clearly provides the worst scheduling delay performance because of the slower traffic adaptation periodicity γ and the large TTI alignment delay, respectively. However, the FDD mode inflicts a lower scheduling delay due to the absence of the TDD switching delay, i.e., $\psi_{\text{tdd}} = \varphi_{\text{tdd}}, = 0$ ms.

URLLC outage latency with the inter-BS CLI:

The inter-BS CLI is considered as the most critical challenge against the 5G-NR dynamic-TDD systems. In this regard, Fig. 7 depicts the CCDF of the URLLC UL latency with the FDD, and TDD duplexing, under CLI-non-free and CLI-free conditions, respectively. The latter case denotes a theoretical baseline, i.e., optimal inter-BS CLI cancellation is assumed, to which we compare the actual performance of the dynamic-TDD systems with CLI coexistence. The URLLC outage latency with unhandled CLI exhibits $+162.19\%$ increase compared to the CLI-free case. This is mainly because of the UL packets getting re-transmitted several times prior to a successful decoding, due to the severe BS-BS CLI, leading to significantly large φ_{td} and $\alpha\varphi_{\text{harq}}$ delays. On another side, the FDD case provides the best UL outage latency, mainly due to the absolute absence of the inter-BS CLI.

VI. Discussions on State-of-the-Art Flexible-FDD

5G-NR dynamic-TDD systems offer a flexible link direction adaptation to the sporadic URLLC packet arrivals. However, throughout the paper, it has been demonstrated an extremely challenging task to achieve the URLLC outage latency and reliability targets in such systems.

In order to overcome the latency challenges of the dynamic-TDD operation, we next briefly consider the option of flexible-FDD operation for unpaired carriers. With the flexible-FDD, a single unpaired carrier frequency is utilized such that some PRBs are used for DL transmissions, while others are concurrently adopted for UL transmissions, as depicted by Fig. 8. Herein, unlike the dynamic-TDD mode, simultaneous DL and UL transmissions are allowed, while still dynamically adjusting the amount of DL and UL frequency resources in line with the BS-specific link selection criterion. For instance, a BS with a buffered traffic ratio ϖ_c of 3:1, adopts 60% : 20% DL-to-UL PRB ratio, while the remaining frequency

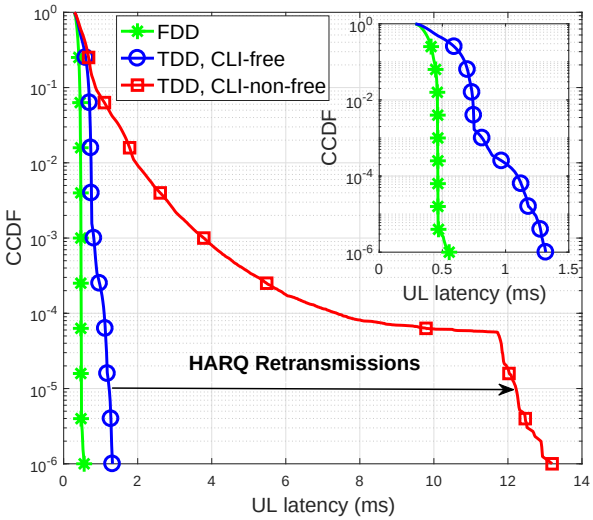

Fig. 7. URLLC outage latency: with CLI for $\Omega = 1.5$ Mbps.

resources are flexibly configured as guard bands. The main advantages of the flexible-FDD over dynamic-TDD mode are as follows: (a) absence of the DL and UL switching delays, i.e., $\psi_{\text{tdd}} = \varphi_{\text{tdd}}, = 0$ ms, and (b) absence of the inter-BS CLI by simpler frequency coordination techniques.

However, flexible-FDD requires efficient self-interference mitigation techniques in practice, in order to cope with the power leakage problem, resulting from the concurrent DL transmissions and UL receptions over the same PRB set. Accordingly, the self-interference mitigation operation is typically implemented as a hybrid process of analog interference suppression and digital interference cancellation. In that sense, a possible variant of a flexible-FDD deployment would therefore be to have BSs operating in the flexible-FDD mode, while connected UEs operate in half-duplex mode, either having an uplink or downlink link activation at time. Thereby, each BS shall simultaneously serve different UEs in opposite/same link directions over partially or fully shared frequency resources; though, without the need of self-interference mitigation capabilities at the UE-side.

VII. Concluding Remarks

In this work, we studied the feasibility of the URLLC outage latency within the 5G new radio dynamic-TDD deployments. The URLLC radio performance is first evaluated under optimal interference-free conditions, with the various system design aspects of the 5G new radio, i.e., offered sporadic packet arrivals, channel sub-carrier spacing, transmission time interval duration, configured and grant-free uplink scheduling. Then, the impact of the inter-cell cross link interference on the achievable URLLC outage latency is identified. Finally, the state-of-the-art flexible-FDD duplexing mode is being introduced towards the upcoming 3GPP standards.

The main insights brought by this paper are summarized as follows: (1) with inter-BS interference-controlled conditions, the 30 kHz sub-carrier spacing (SCS) is proven suitable to satisfy the URLLC 1-ms radio latency target for offered loads

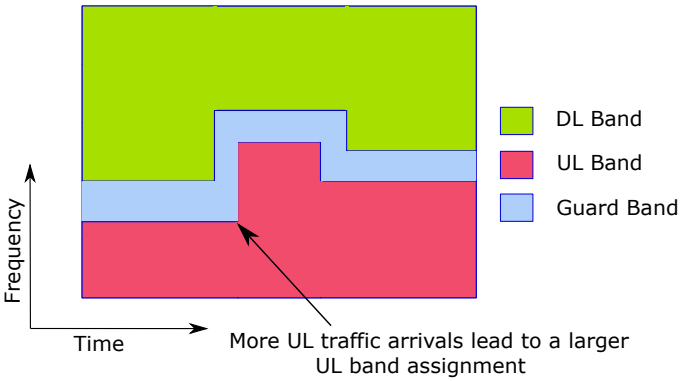

Fig. 8. Flexible-FDD towards upcoming 3GPP 5G standards.

up to 1 Mbps/BS, (2) with higher offered load levels, the SCS of 60 kHz and bandwidth allocation of 20 MHz should be adopted to further reduce the packet segmentation delay, user scheduling delay, TTI duration, UE and BS processing delays, (3) dynamic UL scheduling, the BS and UE processing delays, respectively, introduce a constant delay offset in the URLLC outage latency regardless of the other system design variants, and hence, they should be particularly optimized and (4) adding the BS-BS cross-link interference, the URLLC latency targets are almost not feasible due to the UL capacity blockage.

VIII. Acknowledgments

This work is partly funded by the Innovation Fund Denmark – File: 7038-00009B.

References

[1] Service requirements for the 5G system; Stage-1 (Release 16), 3GPP, TS 22.261, V16.6.0, Dec. 2018.

[2] Service requirements for cyber-physical control applications in vertical domains; Stage-1 (Release 16), 3GPP, TS 22.104, V16.0.0 , Dec. 2018.

[3] A. A. Esswie and K. I. Pedersen, "Opportunistic spatial preemptive scheduling for URLLC and eMBB coexistence in multi-user 5G networks," *IEEE ACCESS.*, vol. 6, pp. 38451-38463, July 2018.

[4] J. Lee et al., "Spectrum for 5G: global status, challenges, and enabling techs," *IEEE Commun. Mag.*, vol. 56, no. 3, pp. 12-18, March 2018.

[5] K. I. Pedersen, G. Berardinelli, F. Frederiksen, P. Mogensen and A. Szufarska, "A flexible 5G frame structure design for FDD cases," *IEEE Commun. Mag.*, vol. 54, no. 3, pp. 53-59, March 2016.

[6] *5G; NR; Physical layer procedures for control*; (Release 15), 3GPP, TS 38.213, V15.3.0, Oct. 2018.

[7] Ali A. Esswie, K.I. Pedersen, and P. Mogensen, "Quasi-dynamic frame coordination for ultra- reliability and low-latency in 5G TDD systems," *in Proc. IEEE ICC*, Shanghai, May 2019.

[8] A. Łukowa and V. Venkatasubramanian, "Performance of strong interference cancellation in flexible UL/DL TDD systems using coordinated muting, scheduling and rate allocation," *in Proc. IEEE WCNC*, Doha, 2016, pp. 1-7.

[9] Ali A. Esswie, and K.I. Pedersen, "Inter-cell radio frame coordination scheme based on sliding codebook for 5G TDD systems," *in Proc. IEEE VTC-spring,* Kuala Lumpur, 2019.

[10] R1-1701146, *Dynamic TDD interference mitigation concepts in NR*, Nokia, Alcatel-Lucent Shanghai Bell, 3GPP RAN1 #88, Feb. 2017.

[11] Ali A. Esswie, and K.I. Pedersen, "Cross link interference suppression by orthogonal projector in 5G dynamic-TDD URLLC systems," *Submitted to IEEE Commun. Lett,* 2019.

[12] R. Abreu, T. Jacobsen, K. Pedersen, G. Berardinelli, and P. Mogensen, "System level analysis of eMBB and grant-free URLLC multiplexing in uplink," *in Proc. IEEE VTC-spring,* Kuala Lumpur, 2019.